Click Here for Full Article

Strong bottom currents and cyclogenesis in Drake Passage

T. K. Chereskin,[1] K. A. Donohue,[2] D. R. Watts,[2] K. L. Tracey,[2]
Y. L. Firing,[1] and A. L. Cutting[2]

Received 20 September 2009; revised 4 November 2009; accepted 10 November 2009; published 2 December 2009.

[1] Observations from 38 bottom-moored Current and Pressure Recording Inverted Echo Sounders (CPIES) deployed in Drake Passage during the 2007–2008 International Polar Year provide unprecedented coverage of near-bottom currents and pressures spanning the entire Antarctic Circumpolar Current. Year-long-mean currents exceed 10 cm s^{-1} north of the Polar Front, and mean directions are not, in general, aligned with the surface fronts. Topographic steering is most evident at the continental margins. Deep eddy kinetic energy (EKE) is maximum at about 200 cm^2 s^{-2} between the Subantarctic and Polar Fronts, coinciding with the location but about one quarter of the value of a maximum in surface EKE. Multiple high-speed current events, with peak speeds of 60–70 cm s^{-1} and lasting 30 to 70 days, are coherent across sites separated by 45 km. The observed spinup of eddies coinciding with meanders in the surface fronts is consistent with deep cyclogenesis. **Citation:** Chereskin, T. K., K. A. Donohue, D. R. Watts, K. L. Tracey, Y. L. Firing, and A. L. Cutting (2009), Strong bottom currents and cyclogenesis in Drake Passage, *Geophys. Res. Lett.*, *36*, L23602, doi:10.1029/2009GL040940.

1. Introduction

[2] The Antarctic Circumpolar Current (ACC) is the largest wind-driven current in the world, with transport estimates ranging from 95 to 184 $\times$ 10^6 m^3 s^{-1} [*Cunningham et al.*, 2003]. It encircles Antarctica and connects all the major oceans. Its importance for global climate springs from both its absolute transport and the eddy fluxes that mix water and properties across it.

[3] The ACC comprises multiple jets, each associated with a density front [*Nowlin et al.*, 1977]. The two strongest fronts are the Subantarctic Front (SAF) and the Polar Front (PF). Mean surface jet speeds are modest, about 50 cm s^{-1} [*Lenn et al.*, 2007]. The large ACC transport results from the vertical extent of the jets as well as from their speed and width. The pressure force exerted by the ACC on topography [*Munk and Palmén*, 1951] is thought to be the main mechanism by which the wind stress is balanced and the ACC transport is set. Bottom friction may also play a role, but it would require mean bottom velocities of around 20 cm s^{-1} to account for the total balance, and such large values are thought to be unrealistic [*Gill*, 1968]. The deep-reaching jets create a difficult environment in which to measure bottom currents, however, so there are relatively few direct estimates.

[4] *Nowlin et al.* [1977], using three-week averaged speeds from an array of current meters, found eastward bottom velocities in the range of −4 to 6 cm s^{-1} in Drake Passage. *Donohue et al.* [2001] found synoptic bottom velocities in the range of 4–10 cm s^{-1} eastward using shipboard acoustic Doppler current profiler (ADCP) measurements to reference geostrophic currents from six Pacific SAF crossings. *Cunningham et al.* [2003] reported instantaneous bottom velocities of 10–20 cm s^{-1} in the ACC downstream of Drake Passage from lowered ADCP observations. *Gille* [2003] estimated ACC bottom currents in the range of 1–3 cm s^{-1} eastward from historical hydrography and subsurface float observations. Her estimates represent a global average but are sensitive to the mapping scale. Time series in the SAF south of Tasmania yielded mean speeds of 2–3 cm s^{-1} eastward at about 3500 dbar [*Phillips and Rintoul*, 2000; *Meinen et al.*, 2002].

[5] The transient eddy field also exhibits strong bottom currents. South of Tasmania, *Tracey et al.* [2006] found deep eastward propagating cyclones and anticyclones beneath the SAF, similar to observations of cyclogenesis in the Gulf Stream [*Watts et al.*, 1995; *Savidge and Bane*, 1999]. Associated with these eddies, *Meinen et al.* [2002] observed peak speeds of about 30 cm s^{-1} in the SAF while *Savidge and Bane* [1999] observed deep "swirl" velocities of 50 cm s^{-1} in the Gulf Stream.

[6] We report on year-long observations of near-bottom currents and pressures from 38 Current and Pressure Recording Inverted Echo Sounders (CPIES) deployed in Drake Passage during the 2007–2008 International Polar Year. One of the long-term goals of this cDrake project is to resolve the seasonal and interannual variability of the total ACC transport over a period of 4 years. Additionally, a local dynamics array (LDA) was deployed between the SAF and PF, where surface variability is maximum [*Lenn et al.*, 2007]. Daily maps of deep streamfunction together with satellite altimetry provide time sequences of the interaction of the meandering SAF and PF and deep eddies.

2. Data and Methods

[7] The CPIES measures bottom pressure, acoustic travel time to the sea surface and back (tau), and currents 50 m above the bottom with an Aanderaa Instruments RCM-11 Doppler current sensor. The cDrake array (Figure 1) consists of a transport line of 20 CPIES spanning 800 km and a LDA of 21 CPIES spanning 120 km cross-stream and 240 km downstream. Sites are laterally coherent; spacing ranges from 45 to 65 km with the closer spacing north of 57.5°S and near topography. The CPIES sampling rates

[1]Scripps Institution of Oceanography, University of California, San Diego, La Jolla, California, USA.
[2]Graduate School of Oceanography, University of Rhode Island, Narragansett, Rhode Island, USA.

Copyright 2009 by the American Geophysical Union.
0094-8276/09/2009GL040940$05.00

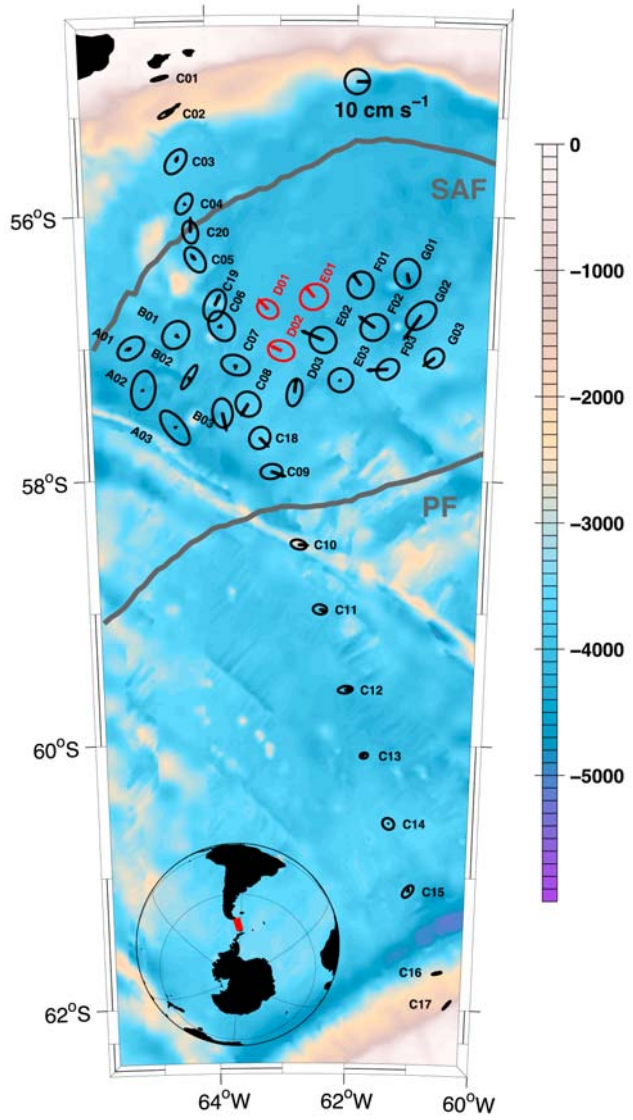

Figure 1. Record-length mean currents and standard deviation ellipses at 50 m above bottom plotted on bathymetry (m) derived from shipboard multibeam measurements and *Smith and Sandwell* [1997]. Time series from 3 recovered instruments (red) are shown in Figure 2. The mean SAF and PF (gray lines) were located following *Lenn et al.* [2008].

were 10 minutes for tau, 30 minutes for pressure, and hourly for velocity.

[8] Data will be collected annually by acoustic telemetry to a ship. Each CPIES internally processes the measurements and saves daily mean values to a file. The pressure and current processing employs a Godin filter to ensure that tides are not aliased. The first year of data was telemetered in late 2008. Due to instrumental issues, 11 instruments were recovered. For consistency, we used daily mean values from the internal telemetry file for recovered sites unless otherwise noted. Currents were corrected in post-processing for local speed of sound and magnetic declination. *Hogg and Frye* [2007] showed that RCM-11 speeds in the range of 0–20 cm s^{-1} are biased low by 1–2 cm s^{-1}. The correction for high speeds is unknown; therefore no correction was applied.

[9] The data revealed three noteworthy phenomena: strong currents, pressure jumps, and instrument tilts. Daily mean speeds in excess of 40 cm s^{-1} were observed, but telemetered speed wraps at 40 cm s^{-1} for better resolution, causing the received speeds to appear low. Unwrapping was done by hand, and consistency checks are described below. Jumps were easily identified as sudden pressure increases (too large to be real ocean signals) caused when the instruments slid down steep topography during strong current events. Jumps exhibited by 4 CPIES were patched by hand editing. Several instruments tipped over during strong current events and then righted themselves after the currents subsided. Pressure records of 13 CPIES were masked for those time periods.

[10] Deep pressures were simultaneously leveled and dedrifted by adjusting records to the same geopotential surface under the assumption that over long periods, near-bottom currents and bottom pressures were in geostrophic balance, and deep currents were vertically uniform [*Donohue et al.*, 2009]. All mapping was done with the optimal interpolation techniques outlined by *Watts et al.* [2001]. Cross-correlations among the measurements determined the 50-km length scale of the Gaussian correlation function employed. Streamfunctions for the combined dedrifting and leveling procedure were determined with 31-day low-pass filtered velocities. For daily maps, multivariate optimally interpolated pressure and velocity were constrained to be geostrophic. Unwrapped current speeds were then reviewed in two ways: First, mapped and measured velocity were compared. Second, mapping was redone excluding current data from each site separately to verify strong current events.

[11] Weekly sea surface height (SSH) anomalies produced by AVISO CLS combined with *Maximenko and Niiler*'s [2005] mean dynamic topography are used to describe surface variability. The SSH contour values for the SAF and the PF identified by *Lenn et al.* [2008] for this dataset were used to define the front locations. Conductivity-temperature-depth (CTD) casts taken at each CPIES site were used to determine the base of the PF pycnocline, which lies at roughly σ_t = 27.7 kg m^{-3}.

3. Results

[12] Fifteen sites have mean speeds in excess of 10 cm s^{-1}, exceeding their standard deviations (Figure 1). These sites are all north of 58°S and lie within or near the LDA. The mean directions in the LDA do not parallel the mean surface fronts determined from SSH; in the eastern LDA, a broad cyclonic pattern is observed (Figure 1).

[13] Mean bottom currents close to and south of the PF approximately parallel it (Figure 1). Speeds at sites C10 to C12 decrease from about 8 to 5 cm s^{-1}. Although the mean current exceeds its standard deviation ellipse only at C10, the means at C11–C12 are significant, since the standard errors in the mean are quite small. Vectors contained within their ellipses indicate no dominant direction. Twenty-eight of the means are significant, using an integral time scale of 45 days to estimate the degrees of freedom.

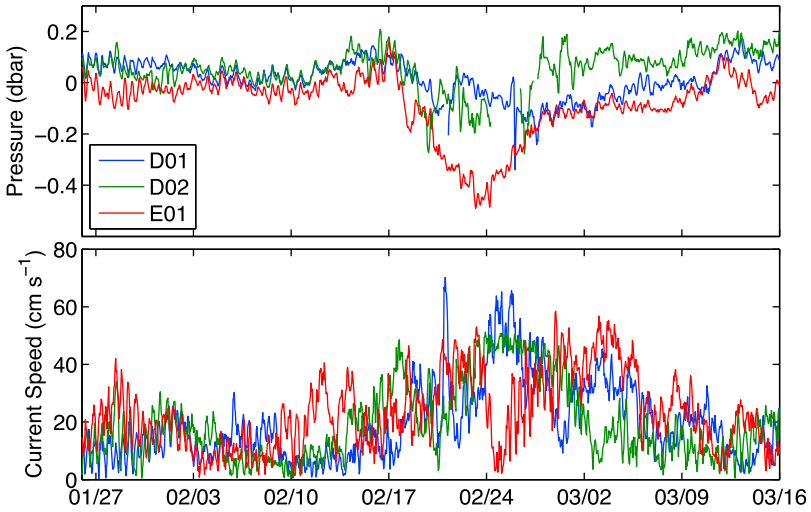

Figure 2. Hourly records from 3 sites (Figure 1) exhibit (top) a strong pressure anomaly and (bottom) swift currents during the cyclogenesis case study (Figure 4).

[14] We found multiple high-speed events in the hourly time series from the 11 recovered sites. During the most energetic event, peak hourly speeds exceeded 55 cm s^{-1} (Figure 2) at several sites. Stronger hourly currents were observed at individual sites during other events. For example, C09 had sustained currents near 70 cm s^{-1} for a 24 hour period. C05 had speeds over 40 cm s^{-1} for 7 days in a row, reaching 60–78 cm s^{-1} for 2 days straight.

[15] Long-term mean surface EKE confirms that a local maximum lies between the fronts and directly within the LDA (Figure 3a). The annual mean deep EKE values peak around 200 cm^2 s^{-2} (Figure 3c) and scale at about one quarter of surface values estimated for the same time interval (Figure 3b).

[16] The large amplitude mean currents and high EKE observed in the LDA are associated with transient eddies that develop in conjunction with large amplitude meanders in the surface fronts. From Nov 2007 to Nov 2008 six such events occurred, varying in length from 30 to 70 days. The strongest event in the year-long record (Figure 4) typifies the time evolution seen in the others. During this event the LDA-averaged deep EKE exceeded 125 cm^2 s^{-2} for 22 consecutive days (12 Feb to 4 Mar), reaching a maximum of 367 cm^2 s^{-2} on 23 Feb (not shown).

[17] On 4 Feb, the SAF and PF were located on the array periphery. Over the next 10 days, the SAF developed a steep crest that moved southeastward nearly 55 km while a deep anticyclone spun up with maximum pressure near 0.28 dbar, daily-averaged swirl speeds near 25 cm s^{-1} and estimated Rossby number *Ro* near −0.15 ($Ro = \zeta/f$ where ζ is relative vorticity and f is the Coriolis parameter). The SAF subsequently retracted quickly back to its nominal mean position.

[18] Also during this event, a PF trough rapidly steepened (4–24 Feb), advancing first eastward and then northward, with a net displacement of 150 km over 20 days while a deep cyclone developed with maximum Ro = 0.4. Peak currents >55 cm s^{-1} swirled around the cyclone while pressure at its center dropped to −0.4 dbar (Figures 2 and 4). Subsequently, a ring pinched off the PF and propagated northward out of the LDA. Hourly current speeds >40 cm s^{-1} persisted for several days while the intense low pressure cell passed through the sites D01, D02 and E01 (Figure 2).

[19] We hypothesize that deep cyclogenesis occurs in response to stretching of the lower-layer during SAF/PF meanders. Conservation of potential vorticity (PV) requires

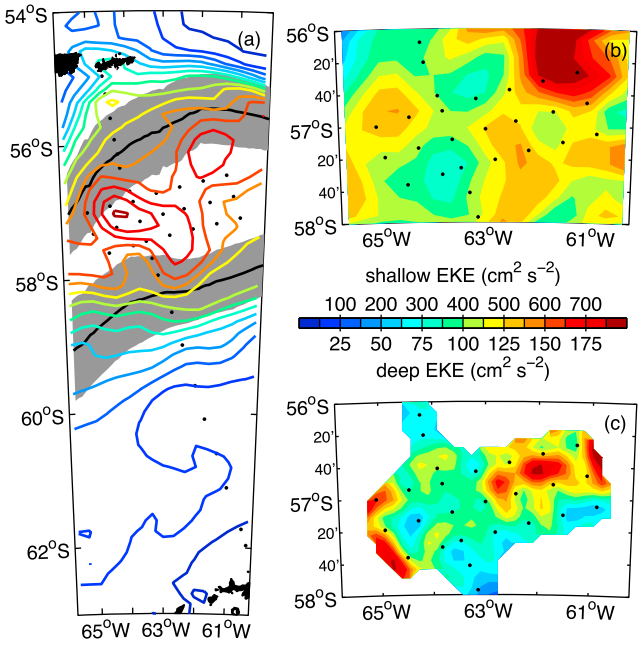

Figure 3. Surface and deep eddy kinetic energy (EKE). Note that there are 2 colorbar scalings corresponding to shallow and deep EKE. Filled dots mark the location of the cDrake array. (a) Long-term mean (14 Oct 1992–18 Feb 2009) altimetric surface EKE (color contours). Gray envelopes show one standard deviation about the mean SAF and PF paths (black lines) for this time period following *Lenn et al.* [2008]. (b) Mean (23 Nov 2007–18 Nov 2008) altimetric surface EKE in the region of the cDrake array. (c) Mean (23 Nov 2007–18 Nov 2008) EKE at 50 m above bottom in the cDrake array estimated from daily streamfunction maps.

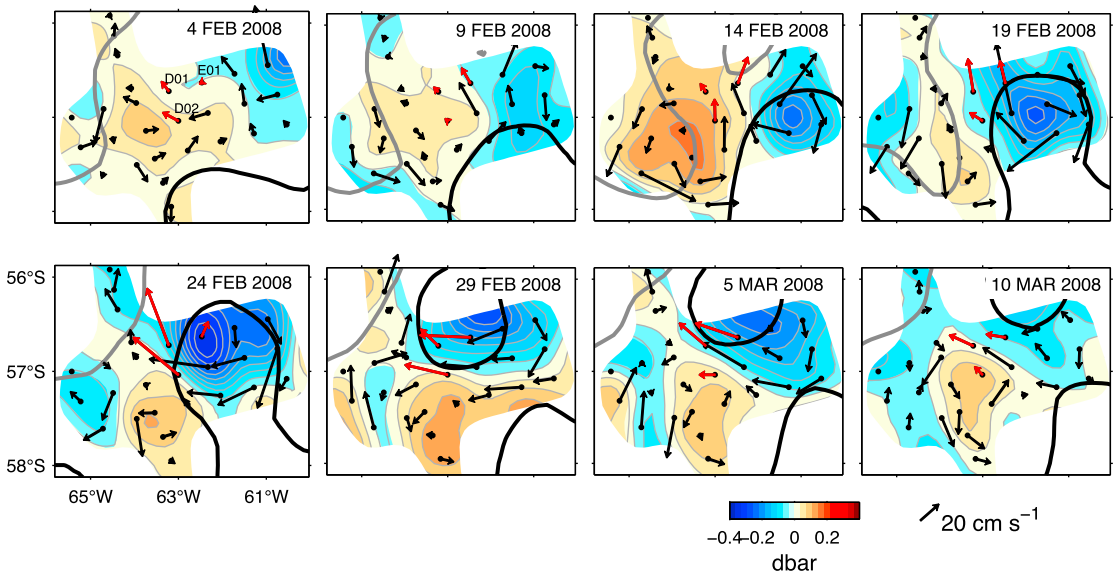

Figure 4. Maps of deep streamfunction during the most energetic cyclogenesis event are shown at 5-day intervals. The daily-averaged near-bottom pressure anomaly field (color-shaded) is contoured at 0.04 dbar intervals. Contours indicate the surface SAF (gray) and PF (black) paths. Filled dots indicate CPIES sites. Daily current vectors are shown; those for the three sites in Figure 2 are in red.

that changes in relative vorticity and lower-layer thickness balance,

$$\frac{D}{Dt}\{PV\} = \frac{D}{Dt}\left\{\frac{f+\zeta}{H_o+h}\right\} = 0,$$

where H_o is the initial lower-layer thickness just before the cyclogenesis and h is the change in lower-layer thickness due to the upper jet meander.

[20] Applying this to observations, we neglect nonlinear advection and calculate relative vorticity from daily streamfunction maps. The lower layer is demarcated between the base of the PF pycnocline and the seafloor. We estimate the change in lower-layer thickness by correlating absolute SSH with PF pycnocline depth, using 44 hydrocasts to fit a linear model with $r^2 = 0.98$. This provides a look-up between SSH and PF pycnocline depth.

[21] At site C08, the linear model predicts that lower-layer thickness decreases by 300 m from its initial thickness of 2750 m during the SAF crest development on 10–16 Feb. Conservation of PV requires the generation of anticyclonic vorticity with $Ro = -0.1$, close to that observed. Similarly at site E02, the model predicts lower-layer thickness increases by 1150 m from its starting value of 2600 m during the PF trough development on 3–19 Feb. PV conservation requires the generation of cyclonic vorticity with $Ro = 0.44$, close to that observed.

4. Conclusions

[22] The cDrake array provided unprecedented coverage of near-bottom pressures and currents across the ACC in Drake Passage. At 15 sites in northern Drake Passage, near-bottom mean currents exceeded 10 cm s^{-1}, larger than previous estimates in the ACC [*Nowlin et al.*, 1977; *Phillips and Rintoul*, 2000; *Meinen et al.*, 2002], and unlike previous observations, the direction did not parallel the mean surface flow as determined from satellite altimetry. Deep EKE was maximum between the SAF and PF, coinciding with the location but about one quarter of the value of maximum surface EKE inferred from altimetry. South of the PF, mean deep currents were smaller (about 5 cm s^{-1}), and the direction generally coincided with the mean surface flow.

[23] Multiple high-speed current events, with peak speeds of 60–70 cm s^{-1} and lasting 30 to 70 days, were coherent across sites separated by 45 km. Daily synoptic streamfunction maps showed the spinup of deep eddies consistent with cyclogenesis. A simple 2-layer model relating lower-layer thickness to surface height suggests that, to lowest order, changes in lower layer thickness compensated changes in relative vorticity. The observations also suggest that bottom friction may play a larger role than previously thought in the ACC momentum balance in Drake Passage.

[24] **Acknowledgments.** The National Science Foundation Office of Polar Programs supported this work under NSF grants ANT-0636493 and ANT-0635437. We thank G. Chaplin, S. Escher, D. Holloway, E. Sousa and A. Troisi, the captains and crew of the RVIB Nathaniel B. Palmer and Raytheon Polar Services for their excellent technical and logistical support during the cruises.

References

Cunningham, S. A., S. G. Alderson, B. A. King, and M. A. Brandon (2003), Transport and variability of the Antarctic Circumpolar Current in Drake Passage, *J. Geophys. Res.*, *108*(C5), 8084, doi:10.1029/2001JC001147.

Donohue, K. A., E. Firing, and S. Chen (2001), Absolute geostrophic velocity within the Subantarctic Front in the Pacific Ocean, *J. Geophys. Res.*, *106*, 19,869–19,882.

Donohue, K. A., D. R. Watts, K. L. Tracey, A. D. Greene, and M. Kennelly (2009), Mapping circulation in the Kuroshio Extension with an array of current and pressure recording inverted echo sounders, *J. Atmos. Oceanic Technol*, doi:10.1175/2009JTECHO686.1, in press.

Gill, A. E. (1968), A linear model of the Antarctic Circumpolar Current, *J. Fluid Mech.*, *32*, 465–488.

Gille, S. T. (2003), Float observations of the Southern Ocean. Part 1: Estimating mean fields, bottom velocities, and topographic steering, *J. Phys. Oceanogr.*, *33*, 1167–1182.

Hogg, N. G., and D. E. Frye (2007), Performance of a new generation of acoustic current meters, *J. Phys. Oceanogr.*, *37*, 148–161.

Lenn, Y. D., T. K. Chereskin, J. Sprintall, and E. Firing (2007), Mean jets, mesoscale variability and eddy momentum fluxes in the surface-layer of the Antarctic Circumpolar Current in Drake Passage, *J. Mar. Res.*, *65*, 27–58.

Lenn, Y.-D., T. K. Chereskin, and J. Sprintall (2008), Improving estimates of the Antarctic Circumpolar Current streamlines in Drake Passage, *J. Phys. Oceanogr.*, *38*, 1000–1010.

Maximenko, N., and P. P. Niiler (2005), Hybrid decade-mean global sea level with mesoscale resolution, in *Recent Advances in Marine Science and Technology*, edited by N. Saxena, pp. 55–59, PACON Int., Honolulu, Hawaii.

Munk, W. H., and E. Palmén (1951), Note on the dynamics of the Antarctic Circumpolar Current, *Tellus*, *3*, 53–55.

Meinen, C. S., D. S. Luther, D. R. Watts, K. L. Tracey, A. D. Chave, and J. Richman (2002), Combining inverted echo sounder and horizontal electric field recorder measurements to obtain absolute velocity profiles, *J. Atmos. Oceanic Technol.*, *19*, 1653–1664.

Nowlin, W. D., Jr., T. Whitworth III, and R. D. Pillsbury (1977), Structure and transport of the Antarctic Circumpolar Current at Drake Passage from short-term measurements, *J. Phys. Oceanogr.*, *7*, 788–802.

Phillips, H. E., and S. R. Rintoul (2000), Eddy variability and energetics from direct current measurements in the Antarctic Circumpolar Current south of Australia, *J. Phys. Oceanogr.*, *30*, 3050–3076.

Savidge, D. K., and J. M. Bane (1999), Cyclogenesis in the deep ocean beneath the Gulf Stream, *J. Geophys. Res.*, *104*, 22,565–22,589.

Smith, W. H. F., and D. T. Sandwell (1997), Global seafloor topography from satellite altimetery and ship depth soundings, *Science*, *277*, 1956–1962.

Tracey, K. L., D. R. Watts, C. S. Meinen, and D. S. Luther (2006), Synoptic maps of temperature and velocity within the Subantarctic Front south of Australia, *J. Geophys. Res.*, *111*, C10016, doi:10.1029/2005JC002905.

Watts, D. R., K. L. Tracey, J. M. Bane, and T. J. Shay (1995), Gulf Stream path and thermocline structure near 74°W and 68°W, *J. Geophys. Res.*, *100*, 18,291–18,312.

Watts, D. R., X. Qian, and K. L. Tracey (2001), Mapping abyssal current and pressure fields under the meandering Gulf Stream, *J. Atmos. Oceanic Technol.*, *18*, 1052–1067.

T. K. Chereskin and Y. L. Firing, Scripps Institution of Oceanography, University of California, San Diego, 9500 Gilman Dr., La Jolla, CA 92093-0230, USA. (tchereskin@ucsd.edu)

A. L. Cutting, K. A. Donohue, K. L. Tracey, and D. R. Watts, Graduate School of Oceanography, University of Rhode Island, 215 South Ferry Rd., Narragansett, RI 02882-1197, USA.